

Holmium-TiO₂ thin film for methanol preparation from photocatalytic reduction of carbon dioxide

E.S. Aazam

Chemistry Department, Faculty of Science, King Abdulaziz University, P.O. Box 80203 Jeddah 21589, Saudi Arabia,
Tel. +966-6400000, Fax +966-2-6952292, email: elhamaazam@gmail.com

Received 12 December 2017; Accepted 31 March 2018

ABSTRACT

Holmium-TiO₂ thin films were fabricated by a sol-gel technique. Holmium-TiO₂ thin films were identified by many characterization techniques, such as UV-Vis, TEM, XPS, BET and XRD. The performance of the holmium-TiO₂ thin film photocatalyst was studied by studying methanol preparation from the photocatalytic reduction of carbon dioxide under visible light. The results showed that holmium-TiO₂ thin film photocatalytic properties can be adjusted by adjusting the holmium weight percent. XPS results revealed that holmium species were present as Ho³⁺ ions due to the presence of a peak for Ho3d_{5/2} at 163.1 eV. BET results reveal that the addition of holmium to TiO₂ led to an increase in the BET surface area of the TiO₂ thin film. Additionally, the addition of holmium species decreased the band gap and increased the e-h recombination rate of titanium dioxide thin films. The highest photocatalytic activity and lowest band gap of the holmium-TiO₂ thin film were achieved at 0.4 wt % holmium. The yield of methanol obtained using a 0.4 wt % Ho/TiO₂ thin film is approximately 32 times that of the TiO₂ thin film. The Holmium-TiO₂ thin film has stable photocatalytic activity until five times for methanol preparation from the photocatalytic reduction of carbon dioxide under visible light.

Keywords: Holmium; Titanium dioxide; Thin film; Methanol; Carbon dioxide reduction

1. Introduction

For the last century, human industrial activities have increased substantially, and as a result, CO₂ emissions have reached unprecedented amounts. Accordingly, the balance between the CO₂ produced and consumed on earth has gradually been disrupted, leading to the global warming phenomenon, which has caused many environmental problems. Therefore, researchers and scientific communities have focused on different routes to reduce the emission of CO₂ or decrease its concentration in the atmosphere for environmental protection. One of the main routes for reducing CO₂ production is its conversion into useful materials [4–6] through different process, such as the electrochemical reduction or artificial photosynthesis, has attracted the interest of scientists worldwide because of the economic and environmental benefits. During this process, electrical

energy is supplied between two electrodes to establish a potential and reduced CO₂ to other forms [4,7–10]. Usually, a variety of products produced from the electrochemical reduction of CO₂ depend on the used catalytic materials and the reaction medium. There are different pathways for electrochemical reduction of CO₂, such as through eight-, six-, four- and two-electron pathways in non-aqueous, gaseous and aqueous phases at different electrode and cell configurations. Electrochemical products for reduction of CO₂ greatly depend on the medium; carbon monoxide, methanol, formaldehyde, formic acid, or formate, oxalic acid or oxalate produced in basic solution, whereas in acidic medium methane, ethanol, or ethylene may produce [11]. One of the great challenges is the conversion of CO₂ into methanol due to their potential applications in various industries. Although methanol is one of the most important precursors for different chemical industries, which is vital to our daily life, such as silicone, paint, and plastics, it is also considered a green fuel due to its low density com-

*Corresponding author.

pared with other fuels [12]. TiO_2 is a widely used photocatalyst because it possesses properties that include chemical stability, nontoxicity, possible reuse, possible incorporation in other materials, and favorable physical properties. Recently, the focus on the application of TiO_2 for the photocatalytic reduction of CO_2 to fuels such as $\text{C}_2\text{H}_5\text{OH}$, CH_3OH and CH_4 , which suffer from the low efficiency due to its wide band gap [23–28]. However, TiO_2 has a wide band gap ($E_g = 3.2$ eV), making it active when used in reactions that involve UV light, which constitute approximately 3%–5% of the solar spectrum; for this, researchers always try to manipulate its structure to narrow the band gap which in turn makes the derived material active in the natural or artificial sunlight. Accordingly, many research works have been devoted to the design of novel photocatalysts for CO_2 reduction with higher selectivity, conversion efficiency, and harvesting visible light [29–37]. Many studies have shown that doping semiconductor oxides greatly enhances their photocatalytic activities for CO_2 reduction. According to my knowledge, there are no reports available to date for the preparation of holmium- TiO_2 thin films or methanol preparation by holmium- TiO_2 thin films. In this research, we report the synthesis of a new holmium- TiO_2 thin film through the sol-gel method, and we will apply this material in a methanol production reaction.

2. Experimental

2.1. Preparation of photocatalysts

Ti precursor, which was used for the preparation of titanium dioxide thin film, is tetrabutyl titanate and holmium precursor, which was used for the preparation of holmium/titanium dioxide thin film is holmium(III) nitrate pentahydrate. The titanium dioxide thin film was prepared by dissolving tetrabutyl titanate in a mixture of propanol and distilled water and the pH of resulting mixture was adjusted by nitric acid to become 2.0 to form stable titania sol. Then, the titania film was formed by dipping the glass plate into titania sol, and the glass plate was calcined at 550°C for 2 h and dried for 2 h at 60°C . The holmium/titanium dioxide thin film samples were prepared by the same method described above in addition to holmium(III) nitrate pentahydrate as a source of holmium, and we used different weight percentages of holmium(III) nitrate pentahydrate to prepare different weight percentages of Ho, such as 0.1, 0.2, 0.3, 0.4 and 0.5 wt %.

2.2. Characterization

X-ray diffractograms of nanocomposites were measured using XRD analysis via $\text{Cu-K}\alpha$ radiation ($\lambda = 1.540\text{\AA}$). A Nova-2000 instrument was adopted for specific surface area determination of nanocomposites through N_2 adsorption at 77 K. Before each measurement, specimens were heated at approximately 250°C for 4 h to remove gases from these specimens. Band gap energies corresponding to the synthesized nanocomposites were measured by applying a spectro-photometer (V-570, JASCO, Japan) via determination of UV-Visible diffuse reflectance spectra (UV-Vis-DRS) in air at ambient temperature within the wavelengths range of 200–800 nm. The morphology and microstructure of the

prepared nanocomposites were investigated using scanning electron microscopy (JEOL-JEM-5410). The elemental analysis of the synthesized specimens was attained using X-ray photoelectron spectroscopy (XPS) of Thermo Scientific K-ALPHA type, England.

2.3. Photocatalytic experiment

The photocatalytic performance of thin film samples was studied for the photocatalytic reduction of CO_2 under visible light. First, the required dose of the photocatalyst was dispersed in 50 ml of 0.08 M sodium bicarbonate solution. The dimension of the reactor used is $30\text{ cm} \times 15\text{ cm} \times 5\text{ cm}$. To remove oxygen from the reaction mixture, nitrogen gas was passed through the reaction mixture for 1 h. To obtain adsorption-desorption equilibrium, the reaction mixture was kept in the dark for 30 min. A 500-W high-pressure Xe lamp was used as the source of irradiation, and we used 2 M NaNO_2 solution to cut off the UV region below 400 nm. The obtained methanol was analyzed using GC-FID. The yield of evolved methanol can be calculated by dividing the total amount of methanol evolved by reaction time. No methanol was detected in any of the tested samples when the reaction was carried out in the dark only. Additionally, no methanol was detected in any of the tested samples when the reaction was carried out using the source of irradiation only.

3. Results and discussion

3.1. Characterizations of thin film samples

XRD patterns of TiO_2 and Ho/ TiO_2 thin film samples are shown in Fig. 1. The results demonstrate that the phase of the thin film samples is the anatase titanium dioxide phase and that there are no peaks for holmium or holmium oxide due to the high dispersion of holmium above titanium dioxide or holmium below the detection border of XRD.

Fig. 2. TEM image of the 0.4 wt % Ho/ TiO_2 thin film sample. The results reveal that the surface of the thin film is homogenous and smooth.

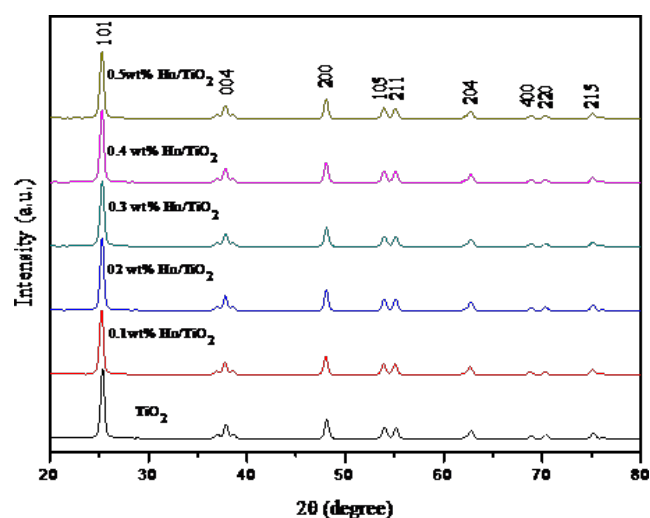


Fig. 1. XRD patterns of TiO_2 and Ho/ TiO_2 thin film samples.

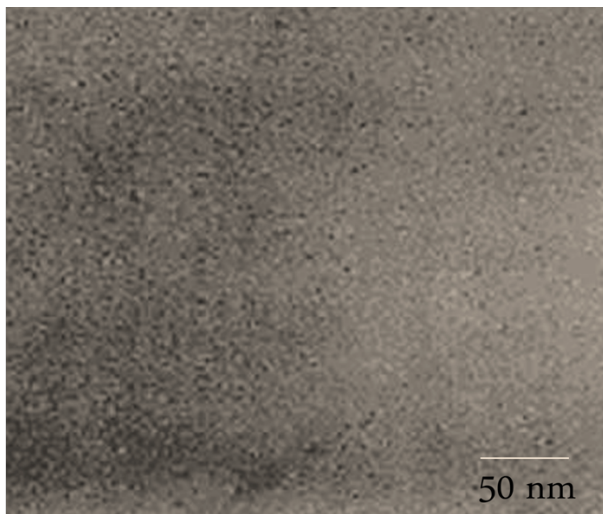


Fig. 2. TEM image of a 0.4 wt % Ho/TiO₂ film sample.

XPS spectra for Ti2P, O1s, and Ho3d for the 0.4 wt % Ho/TiO₂ film sample are shown in Figs. 3A, B and C, respectively. The results reveal that titanium species were present as Ti⁴⁺ ions due to the presence of two peaks for Ti 2p_{3/2} and Ti 2p_{1/2} at 459.1 and 464.4 eV, respectively, as shown in Fig. 3A. Additionally, oxygen species were present as O²⁻ ions due to the presence of a peak for O1s at 529.9 eV, as shown in Fig. 3B. Therefore, TiO₂ is the formed phase due to the presence of Ti⁴⁺ and O²⁻ ions. Holmium species were present as Ho³⁺ ions due to the presence of a peak for Ho3d_{5/2} at 163.1 eV, as shown in Fig. 3C.

3.2. Characterizations of surface area

Table 1 shows the BET surface area of the TiO₂ and Ho/TiO₂ thin film samples. The S_{BET} values for TiO₂, 0.1 wt % Ho/TiO₂, 0.2 wt % Ho/TiO₂, 0.3 wt % Ho/TiO₂, 0.4 wt % Ho/TiO₂, and 0.5 wt % Ho/TiO₂ are 60, 65, 75, 88, 91 and 93 m²/g, respectively. Therefore, the Ho/TiO₂ thin film samples have a surface area higher than that of the TiO₂ sample.

3.3. Characterizations of optical properties

UV-Vis spectra of UV-Vis spectra of TiO₂ and Ho/TiO₂ thin film samples (Fig. 4) reveal a redshift of absorption edges of TiO₂ toward higher wavelengths going from Ho addition. The band gap energies of TiO₂, 0.1 wt % Ho/TiO₂, 0.2 wt % Ho/TiO₂, 0.3 wt % Ho/TiO₂, 0.4 wt % Ho/TiO₂ and 0.5 wt % Ho/TiO₂ samples, which calculated from their respective UV-Vis spectra were 3.2, 2.72, 2.65, 2.57, 2.49 and 2.47 eV, respectively. Therefore, increase wt % of Ho from 0 to 0.4 wt % decrease band gap energy of TiO₂ from 3.2 to 2.49 eV, respectively. Additionally, we noticed that a high wt % of Ho (above 0.4 wt %) has no significant effect on the band gap energy of TiO₂. Therefore, the optimum wt % of Ho is 0.4 wt %.

PI spectra of TiO₂ and Ho/TiO₂ thin film samples (Fig. 5) show a peak intensity decrease in the following order: TiO₂ > 0.1 wt % Ho/TiO₂ > 0.2 wt % Ho/TiO₂ > 0.3 wt % Ho/TiO₂ > 0.4 wt % Ho/TiO₂ > 0.5 wt % Ho/TiO₂.

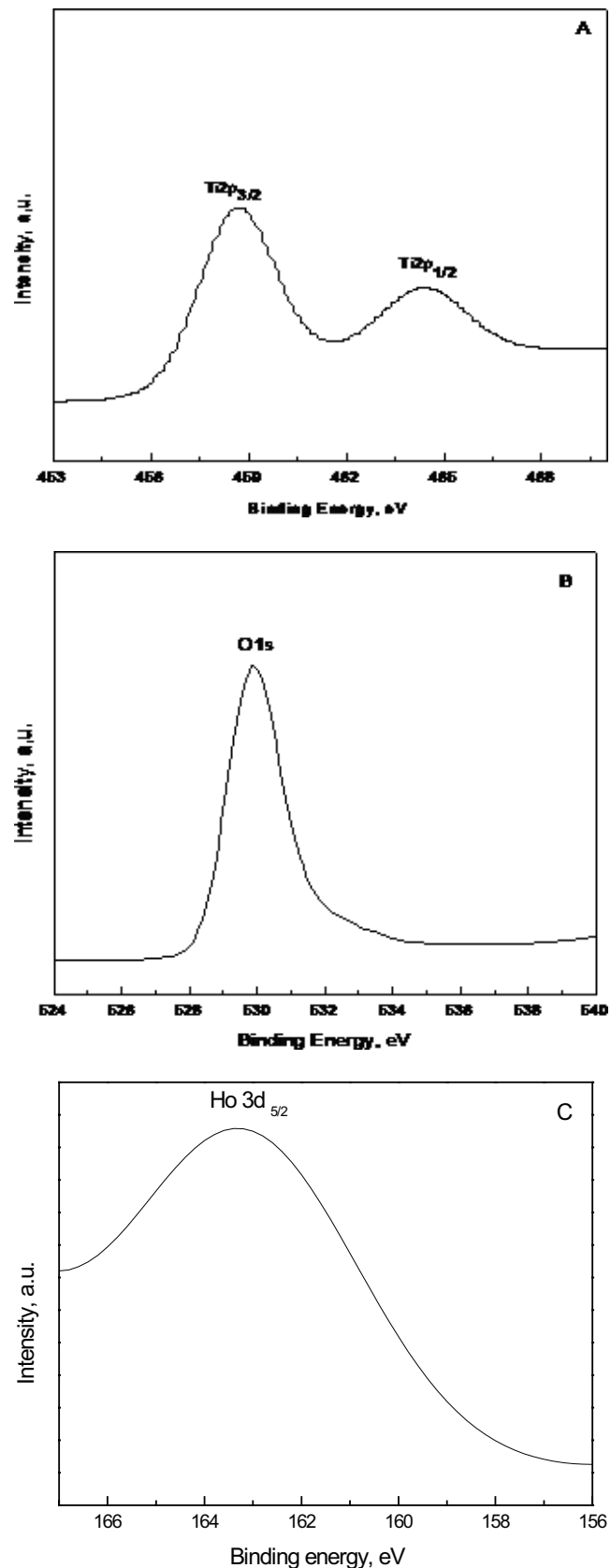


Fig. 3. XPS spectra for Ti2P(A); O1s(B) and Ho3d (C) for the 0.4 wt % Ho/TiO₂ film sample.

Table 1
BET surface area of TiO₂ and Ho/TiO₂ thin film samples

Samples	S _{BET} (m ² /g)
TiO ₂	60
0.1 wt Ho/TiO ₂	65
0.2 wt Ho /TiO ₂	75
0.3 wt Ho /TiO ₂	88
0.4 wt Ho /TiO ₂	91
0.5 wt Ho /TiO ₂	93

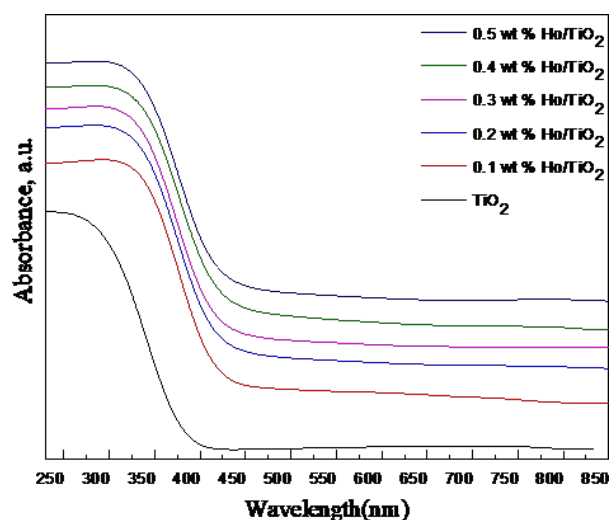


Fig. 4. UV-Vis absorption spectra of TiO₂ and Ho/TiO₂ thin film samples.

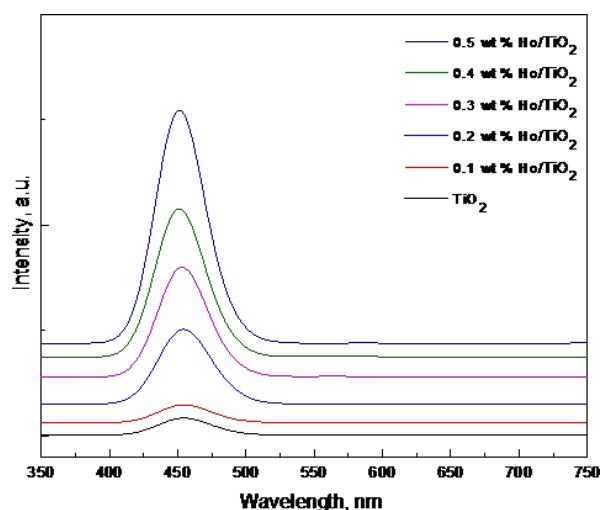


Fig. 5. PL spectra of TiO₂ and Ho/TiO₂ thin film samples.

3.4. Evolution of photocatalytic performance

The type of photocatalyst and recycling and reuse of 0.4 wt % Ho/TiO₂ photocatalyst were studied to measure the photocatalytic performance for methanol production under visible light conditions.

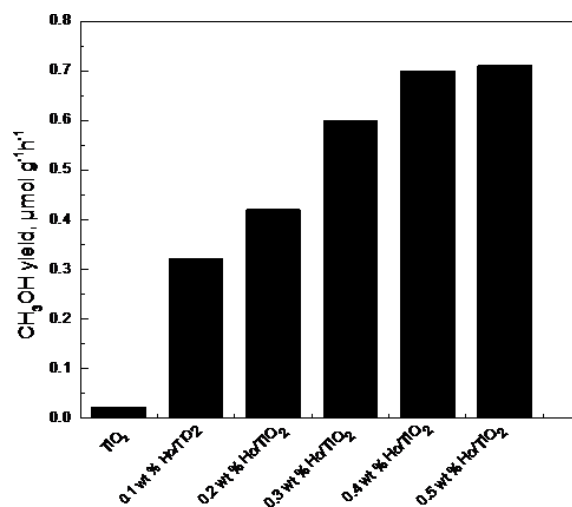


Fig. 6. Effect of the Ho wt % on the photocatalytic activity of TiO₂ and Ho/TiO₂ thin film samples for carbon dioxide photocatalytic reduction.

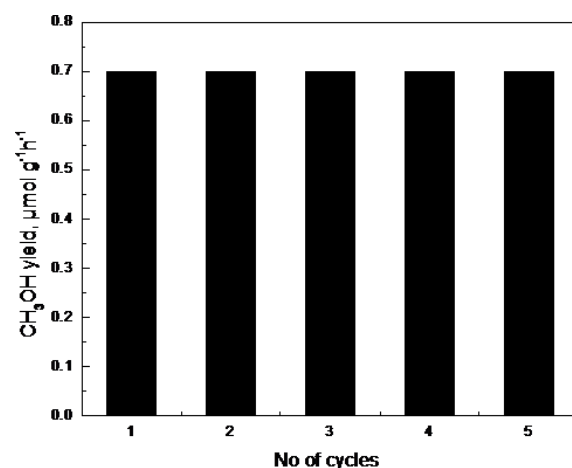


Fig. 7. Recycling and reuse of 0.4 wt % Ho/TiO₂ photocatalysts for carbon dioxide photocatalytic reduction.

The effect of the type of photocatalyst on methanol production was studied. Fig. 6 shows the effect of the type of photocatalyst on methanol production. The TiO₂ sample has almost no photocatalytic activity, as TiO₂ absorbs in the UV region, and the reaction was carried out under visible light. The yield of the Ho/TiO₂ samples for methanol preparation was increased from 0.022 to 0.7 μmol g⁻¹ h⁻¹, respectively, due to the decrease in the band gap of TiO₂ from 3.20 to 2.49 eV by the addition of different wt % of Ho from 0 to 0.4 wt%. Additionally, we noticed that a high wt % of Ho (above 0.4 wt %) has no significant effect on the photocatalytic activity of TiO₂. Therefore, the optimum wt % of Ho is 0.4 wt %, which agrees with previous work [38,39].

Recycling and reuse of 0.4 wt % Ho/TiO₂ photocatalyst on methanol preparation was studied. Fig. 7 shows the recycling and reuse of 0.4 wt % Ho/TiO₂ photocatalyst on methanol preparation. It is clear that the 0.4 wt % Ho/TiO₂ photocatalyst has photocatalytic stability and can be used and recycled many times.

4. Conclusions

In summary, a Holmium-TiO₂ thin film was fabricated by a sol-gel technique. The performance of the holmium-TiO₂ thin film photocatalyst was studied by studying methanol preparation from the photocatalytic reduction of carbon dioxide under visible light. The results showed that holmium-TiO₂ thin film photocatalytic properties can be adjusted by adjusting the holmium weight percent. The highest photocatalytic activity and lowest band gap of the holmium-TiO₂ thin film were achieved at 0.4 wt % holmium. The yield of methanol obtained using a 0.4 wt % Ho/TiO₂ thin film is approximately 32 times that of the TiO₂ thin film. The Holmium-TiO₂ thin film has stable photocatalytic activity until five times for methanol preparation from the photocatalytic reduction of carbon dioxide under visible light.

Acknowledgments

This Project was funded by the Deanship of Scientific Research (DSR) at King Abdulaziz University, Jeddah, under grant no.(G-53-247-438). The authors therefore acknowledge with thanks DSR for technical and financial support.

References

- [1] P. Heptonstall, A. Lyngfelt, Z. Makuch, E. Mangano, R.T.J. Porter, M. Pourkashanian, G.T. Rochelle, N. Shah, J.G. Yao, P.S. Fenell, Carbon capture and storage update, *Energy Environ. Sci.*, 7 (2014) 130–189.
- [2] J. Albo, A. Irabien, Non-dispersive absorption of CO₂ in parallel and cross-flow membrane modules using EMISE, *J. Chem. Technol. Biot.*, 87 (2012) 1502–1507.
- [3] J. Albo, P. Luis, A. Irabien, Absorption of coal combustion flue gases in ionic liquids using different membrane contactors, *Desal. Water Treat.*, 27(1–3) (2011) 54–59.
- [4] D.T. Whipple, P.J.A. Kenis, Prospects of CO₂ utilization via direct heterogeneous electrochemical reduction, *J. Phys. Chem. Lett.*, 1 (2010) 3451–3458.
- [5] M. Alvarez-Guerra, S. Quintanilla, A. Irabien, Conversion of carbon dioxide into formate using a continuous electrochemical reduction process in a lead cathode, *Chem. Eng. J.*, 207 (2012) 278–284.
- [6] J. Albo, M. Alvarez-Guerra, P. Castaño, A. Irabien, Towards the electrochemical conversion of carbon dioxide into methanol, *Green Chem.*, 17 (2015) 2304–2324.
- [7] M. Gattrell, N. Gupta, A. Co, Electrochemical reduction of CO₂ to hydrocarbons to store renewable electrical energy and upgrade biogas, *Energy Convers. Manage.*, 48 (2007) 1255–165.
- [8] C. Oloman, H. Li, Electrochemical processing of carbon dioxide, *Chem. Sus. Chem.*, 1 (2008) 385–391.
- [9] N.S. Lewis, D.G. Nocera, Powering the planet: Chemical challenges in solar energy utilization, *Proc. Natl. Acad. Sci. USA*, 103 (2006) 15729–15735.
- [10] G.A. Olah, A. Goepfert, G.K.S. Prakash, Chemical recycling of carbon dioxide to methanol and dimethyl ether: from greenhouse gas to renewable, environmentally carbon neutral fuels and synthetic hydrocarbons, *J. Org. Chem.*, 74 (2009) 487–498.
- [11] J. Qiao, Y. Liu, F. Hong, J. Zhang, A review of catalysts for the electroreduction of carbon dioxide to produce low-carbon fuels, *Chem. Soc. Rev.*, 43 (2014) 631–675.
- [12] R.H. Perry, D.W. Green, *Perry's Chemical Engineers' Handbook*, McGraw-Hill, New York, 1999.
- [13] M. Spichiger-Ulmann, J. Augustynski, Electrochemical reduction of bicarbonate ions at a bright palladium cathode, *J. Chem. Soc., Faraday Trans.*, 81 (1985) 713–716.
- [14] M. Azuma, K. Hashimoto, M. Watanabe, T. Sakata, Electrochemical reduction of carbon dioxide to higher hydrocarbons in a KHCO₃ aqueous solution, *J. Electroanal. Chem.*, 294 (1990) 299–303.
- [15] S. Nakagawa, A. Kudo, M. Azuma, T. Sakata, Effect of pressure on the electrochemical reduction of CO₂ on Group VIII metal electrodes, *J. Electroanal. Chem.*, 308 (1991) 339–343.
- [16] K. Ohkawa, K. Hashimoto, A. Fujishima, Y. Noguchi, S. Nakayama, Electrochemical reduction of carbon dioxide on hydrogenstoring materials: Part 1. The effect of hydrogen absorption on the electrochemical behavior on palladium electrodes, *J. Electroanal. Chem.*, 345 (1993) 445–456.
- [17] K. Ohkawa, Y. Noguchi, S. Nakayama, K. Hashimoto, A. Fujishima, Electrochemical reduction of carbon dioxide on hydrogen-storing materials.: Part II. Copper-modified palladium electrode, *J. Electroanal. Chem.*, 348 (1993) 459–464.
- [18] K. Ohkawa, Y. Noguchi, S. Nakayama, K. Hashimoto, A. Fujishima, Electrochemical reduction of carbon dioxide on hydrogen-storing materials: Part 3. The effect of the absorption of hydrogen on the palladium electrodes modified with copper, *J. Electroanal. Chem.*, 69 (1994) 165–173.
- [19] B.I. Podlovchenko, E.A. Kolyadko, S. Lu, Electroreduction of carbon dioxide on palladium electrodes at potentials higher than the reversible hydrogen potential, *J. Electroanal. Chem.*, 373 (1994) 185–187.
- [20] D.H. Gibson, The organometallic chemistry of carbon dioxide, *Chem. Rev.*, 96 (1996) 2063–2096.
- [21] X. Yin, J.R. Moss, Recent developments in the activation of carbon dioxide by metal complexes, *Coord. Chem. Rev.*, 181 (1999) 27–59.
- [22] H. Taketa, O. Ishitani, Development of efficient photocatalytic systems for CO₂ reduction using mononuclear and multinuclear metal complexes based on mechanistic studies, *Coord. Chem. Rev.*, 254 (2010) 346–354.
- [23] T. Inoue, A. Fujishima, S. Konishi, K. Honda, Photoelectrocatalytic reduction of carbon dioxide in aqueous suspensions of semiconductor powders, *Nature*, 277 (1979) 637–638.
- [24] V.P. Indrakanti, J.D. Kubicki, H.H. Schobert, Photoinduced activation of CO₂ on Ti-based heterogeneous catalysts: Current state, chemical physics-based insights and outlook, *Energy Environ. Sci.*, 2 (2009) 745–758.
- [25] N.M. Dimitrijevic, B.K. Vijayan, O.G. Poluektov, T. Rajh, K.A. Gray, H. He, P. Zapol, Role of water and carbonates in photocatalytic transformation of CO₂ to CH₄ on titania, *J. Am. Chem. Soc.*, 133 (2011) 3964–3971.
- [26] M. Anpo, J.M. Thomas, Single-site photocatalytic solids for the decomposition of undesirable molecules, *Chem. Commun.*, (2006) 3273–3278.
- [27] T.V. Nguyen, J.C.S. Wu, C.H. Chiou, Photoreduction of CO₂ over Ruthenium dye-sensitized TiO₂-based catalysts under concentrated natural sunlight, *Catal. Commun.*, 9 (2008) 2073–2076.
- [28] C. Wang, R.L. Thompson, J. Baltrus, C. Matranga, Visible light photoreduction of CO₂ Using CdSe/Pt/TiO₂ heterostructured catalysts, *J. Phys. Chem. Lett.*, 1 (2010) 48–53.
- [29] L. Jia, J. Li, W. Fang, H. Song, Q. Li, Y. Tang, Visible-light-induced photocatalyst based on C-doped LaCoO₃ synthesized by novel microorganism chelate method, *Catal. Commun.*, 10 (2009) 1230–1234.
- [30] P.W. Pan, Y.W. Chen, Photocatalytic reduction of carbon dioxide on NiO/InTaO₄ under visible light irradiation, *Catal. Commun.*, 8 (2007) 1546–1549.
- [31] J. Pan, X. Wu, L.Z. Wang, G. Liu, G.Q. Lu, H.M. Chen, Synthesis of anatase TiO₂ rods with dominant reactive {010} facets for the photoreduction of CO₂ to CH₄ and use in dye-sensitized solar cells, *Chem. Commun.*, 47 (2011) 8361–8363.
- [32] S. Yan, S. Ouyang, J. Gao, M. Yang, J. Feng, X. Fan, L. Wan, Z. Li, J.H. Ye, Y. Zhou, Z.G. Zou, A room-temperature reactive-tem-plate route to mesoporous ZnGa₂O₄ with improved photocatalytic activity in reduction of CO₂, *Angew. Chem. Int. Ed.*, 49 (2010) 6400–6404.

- [33] S. Sato, T. Arai, T. Morikawa, K. Uemura, T.M. Suzuki, H. Tanaka, T. Kajino, Selective CO₂ conversion to formate conjugated with H₂O oxidation utilizing semiconductor/complex hybrid photocatalysts, *J. Am. Chem. Soc.*, 133 (2011) 15240.
- [34] C. Wang, R.L. Thompson, P. Ohodnicki, J. Baltrus, C. Matranga, Size-dependent photocatalytic reduction of CO₂ with PbS quantum dot sensitized TiO₂ heterostructured photocatalysts, *J. Mater. Chem.*, 21 (2011) 13452–13457.
- [35] H. Li, Y. Lei, Y. Huang, Y. Fang, Y. Xu, L. Zhu, X. Li, Photocatalytic reduction of carbon dioxide to methanol by Cu₂O/SiC nanocrystallite under visible light irradiation, *J. Nat. Gas Chem.*, 20 (2011) 145–150.
- [36] H. Shi, T. Wang, J. Chen, C. Zhu, J. Ye, Z. Zou, Photoreduction of carbon dioxide over NaNbO₃ nanostructured photocatalysts, *Catal. Lett.*, 141 (2011) 525–530.
- [37] Y. Liu, B. Huang, Y. Dai, X. Zhang, X. Qin, M. Jiang, Selective ethanol formation from photocatalytic reduction of carbon dioxide in water with BiVO₄ photocatalyst, *Catal. Commun.*, 11 (2009) 210–213.
- [38] J. Albo, D. Vallejo, G. Beobide, O. Castillo, P. Castano, A. Irabien, Copper-based metal–organic porous materials for CO₂ electrocatalytic reduction to alcohols, *Chem. Sus. Chem.*, 10(6) (2017) 1100–1109.
- [39] P. Castano, Pyridine-based aqueous solutions enhance methanol electrosynthesis from CO₂, *J. CO₂ Util.*, 18 (2017) 164–172.